Mayhew, S. G., Foust, G. P., & Massey, V. (1969) *J. Biol. Chem. 244*, 803–810.
Meyer, T. E., Przysiecki, C. T., Watkins, J. A., Bhattacharyya, A., Simondsen, R. P., Cusanovich, M. A., & Tollin, G. (1983) *Proc. Natl. Acad. Sci. U.S.A. 80*, 6740–6744.
O'Donnell, M. E., & Williams, C. H., Jr. (1983) *J. Biol. Chem. 258*, 13795–13805.
Ohnishi, T., King, T. E., Salerno, J. C., Blum, H., Bowyer, J. R., & Maida, T. (1981) *J. Biol. Chem. 256*, 5577–5582.
Przysiecki, C. T., Bhattacharyya, A. K., Tollin, G., & Cusanovich, M. A. (1985) *J. Biol. Chem. 260*, 1452–1458.
Shin, M., Sakihama, N., Nijmi, K., & Oshino, R. (1982) *Flavins Flavoproteins, Proc. Int. Symp., 6th*, 672–674.
Simondsen, R. P., & Tollin, G. (1983) *Biochemistry 22*, 3008–3016.
Simondsen, R. P., Weber, P. C., Salemme, F. R., & Tollin, G. (1982) *Biochemistry 21*, 6366–6375.
Smith, M. M., Smith, W. H., & Knaff, D. B. (1981a) *Biochim. Biophys. Acta 592*, 303–313.
Smith, M. M., Smith, W. H., & Knaff, D. B. (1981b) *Biochim. Biophys. Acta 635*, 405–411.
Stankovich, M. A., Schopfer, L. M., & Massey, V. (1978) *J. Biol. Chem. 253*, 4971–4979.
Stombaugh, N. A., Sundquist, J. E., & Orme-Johnson, W. J. (1976) *Biochemistry 15*, 2633–2641.
Tollin, G., Meyer, T. E., & Cusanovich, M. A. (1982) *Biochemistry 21*, 3849–3856.
Tsukihara, T., Fukuyama, K., Nakamura, M., Katsube, Y., Tanaka, N., Kakudo, M., Wada, K., Hase, T., & Matsubara, H. (1981) *J. Biochem. (Tokyo) 90*, 1763–1773.
Weber, P. C., & Tollin, G. (1985) *J. Biol. Chem. 260*, 5568–5573.
Zanetti, G., & Curti, B. (1980) *Methods Enzymol. 69*, 250–255.

# Interaction of Spin-Labeled Nicotinamide Adenine Dinucleotide Phosphate with Chicken Liver Fatty Acid Synthase†

Soo-Ik Chang and Gordon G. Hammes*
*Department of Chemistry, Cornell University, Ithaca, New York 14853-1301*
*Received February 5, 1986; Revised Manuscript Received April 10, 1986*

ABSTRACT: The spatial relationships between the four reduced nicotinamide adenine dinucleotide phosphate (NADPH) binding sites on chicken liver fatty acid synthase were explored with electron paramagnetic resonance (EPR) and spin-labeled analogues of $NADP^+$. The analogues were prepared by reaction of $NADP^+$ with 2,2,5,5-tetramethyl-1-oxy-3-pyrroline-3-carboxylic acid, with 1,1′-carbonyldiimidazole as the coupling reagent. Several esterification products were characterized, and the interaction of the $N_{3'}$ ester of $NADP^+$ with the enzyme was examined in detail. Both $^1H_{13}$,$^{14}N$ and $^2H_{13}$,$^{15}N$ spin-labels were used: the EPR spectrum was simpler, and the sensitivity greater, for the latter. The spin-labeled $NADP^+$ is a competitive inhibitor of NADPH in fatty acid synthesis, and an EPR titration of the enzyme with the modified $NADP^+$ indicates four identical binding sites per enzyme molecule with a dissociation constant of 124 $\mu$M in 0.1 M potassium phosphate and 1 mM ethylenediaminetetraacetic acid (pH 7.0) at 25 °C. The EPR spectra indicate the bound spin-label is immobilized relative to the unbound probe. No evidence for electron–electron interactions between bound spin-labels was found with the native enzyme, the enzyme dissociated into monomers, or the enzyme with the enoyl reductase sites blocked by labeling the enzyme with pyridoxal 5′-phosphate. Furthermore, the EPR spectrum of bound ligand was the same in all cases. This indicates that the bound spin-labels are at least 15 Å apart, that the environment of the spin-label at all sites is similar, and that the environment is not altered by major structural changes in the enzyme. The EPR spectra were simulated with a stochastic Brownian motion model, and the rotational correlation times were found to be similar in the presence and absence of glycerol, indicating local rotation of the bound spin-label. The rotational correlation time at 25 °C is 27 ns, and its activation energy is 2.3 kcal/mol.

Animal fatty acid synthase is one of the most complex multienzyme complexes in the animal kingdom, and the molecular structure of the enzyme is not yet known. The chicken liver enzyme contains seven different enzyme activities and consists of two identical polypeptide chains per molecule [cf. Wakil et al. (1983)]. The structure of the chicken liver enzyme ($M_r$ ~500 000) has been extensively probed with proteolytic enzymes (Wakil et al., 1983; Tsukamoto et al., 1983): the enzyme has three distinct structural domains. The dehydratase, the β-ketoacyl reductase, the enoyl reductase, and the 4′-phosphopantetheine are in one domain ($M_r$ ~107 000). The other two structural domains contain the acetyl and malonyl transacylases ($M_r$ ~127 000) and the thioesterase ($M_r$ ~33 000), respectively. The β-ketoacyl synthase requires the interaction of two different structural domains, but the catalytic site is in the same structural domain as the transacylases.

The mechanism of action of the multienzyme complex involves initiation of the fatty acid chain by transfer of an acetyl group to the enzyme. The chain is then lengthened in two-carbon increments by the transfer of a malonyl residue to the enzyme. Each malonyl is condensed onto the growing chain (β-ketoacyl synthase); the resulting ketone is reduced to an

† This work was supported by grants from the National Institutes of Health (GM 13292) and the National Science Foundation (PCM 8120818).

0006-2960/86/0425-4661$01.50/0 

alcohol by NADPH[1] ($\beta$-ketoacyl reductase); the alcohol is dehydrated (dehydratase); and the resulting carbon–carbon double bond is reduced by NADPH (enoyl reductase). When palmitic acid is formed, a thioesterase releases the product from the enzyme. The elementary steps in the reaction mechanism, the detailed stereochemistry, and the nature of the enzyme-bound reaction intermediates have been explored [cf. Hammes (1985), Cognet and Hammes (1985), Anderson and Hammes (1984, 1985), and Yuan and Hammes (1985)].

In this study, the spatial relationships between the two reductase sites were examined with a spin-labeled analogue of $NADP^+$. The results obtained indicate that four NADPH binding sites on the enzyme are at least 15 Å apart and that the EPR spectrum of the bound spin-labeled analogue of $NADP^+$ is identical at all four sites. Furthermore, the EPR spectrum is not altered when the enzyme is dissociated into monomers or when the enoyl reductase sites are specifically blocked. The bound spin-label displays rapid, but restricted, rotation on the enzyme surface.

## Materials and Methods

*Chemicals.* NADPH, $NADP^+$, acetyl-CoA, malonyl-CoA, pyridoxal 5′-phosphate, $NaBH_4$, crotonyl-CoA, D-glucose 6-phosphate, D-glucose-6-phosphate dehydrogenase (from Baker's yeast, type VII), acetoacetyl-CoA, and 1,1′-carbonyldiimidazole were from Sigma Chemical Co. [$^1H_{13}$,$^{14}N$]-2,2,5,5-Tetramethyl-1-oxy-3-pyrroline-3-carboxylic acid was from Molecular Probes, Inc.; [$^2H_{13}$,$^{15}N$]-2,2,5,5-tetramethyl-1-oxy-3-pyrroline-3-carboxylic acid was from MSD Isotopes; and DEAE-Sephadex A-25 was from Pharmacia Fine Chemicals. Silica gel plates for thin-layer chromatography with fluorescent indicator were from Macherey-Nagel. All other chemicals were high-quality commercial grades, and all solutions were prepared with deionized water.

Concentrations of acetyl-CoA, malonyl-CoA, and acetoacetyl-CoA were determined with extinction coefficients of $1.5 \times 10^4$ $M^{-1}$ $cm^{-1}$ at 260 nm (P-L Biochemical Circular OR-10). Concentrations of NADPH and crotonyl-CoA were determined with extinction coefficients of $6.22 \times 10^4$ $M^{-1}$ $cm^{-1}$ at 340 nm (P-L Biochemical Circular OR-10) and $1.9 \times 10^4$ $M^{-1}$ $cm^{-1}$ at 260 nm (Vernon & Hsu, 1984), respectively.

*Fatty Acid Synthase Preparation and Assay.* The enzyme was prepared from chicken livers and assayed as previously described (Yuan & Hammes, 1985; Cox & Hammes, 1983). Fractions with a specific activity greater than 1.6 $\mu$mol of NADPH/(min·mg) were collected. The final enzyme concentration was greater than 8 mg/mL. The protein concentration was determined by measurement of the absorbance at 280 nm and by use of an extinction coefficient for fatty acid synthase of $4.82 \times 10^5$ $M^{-1}$ $cm^{-1}$ (Hsu & Yun, 1970). The 10 mM dithiothreitol and 10% glycerol (w/v) necessary for storage of the purified enzyme were removed by passage of the enzyme through a 3-mL Sephadex G-50 centrifuge column (Penefsky, 1977), preequilibrated with either 0.1 M potassium phosphate and 1 mM EDTA (pH 7.0) or 5 mM Tris, 35 mM glycine, and 1 mM ETA (pH 8.3). For EPR measurements, the enzyme was concentrated in a microconcentrator (Amicon, Model 4205).

The fatty acid synthase was dissociated into monomers as previously described (Kumar & Porter, 1971; Yun & Hsu, 1972; Anderson & Hammes, 1983).

The enzyme was modified with pyridoxal 5′-phosphate by the method of Poulose and Kolattukudy (1980), as previously described (Cardon & Hammes, 1983). Pyridoxal 5′-phosphate was added to fatty acid synthase (8–9 mg/mL) to a final concentration of 2 mM, and the adduct was reduced with $NaBH_4$ (final concentration, 10 mM). For control experiments, the enzyme was treated similarly, but pyridoxal 5′-phosphate was omitted. The overall activity of the enzyme was assayed by adding 20 $\mu$L of a mixture of 4.6 mM malonyl-CoA and 2.3 mM acetyl-CoA to 0.9 mL of 0.1 M potasssium phosphate (pH 7.0), 1 mM EDTA, and 100 $\mu$M NADPH containing a known amount of enzyme at 25 °C. Assays of the dissociated enzyme were carried out at 4 °C. The ketoacyl reductase was assayed by adding 20 $\mu$L of 9.88 mM acetoacetyl-CoA to 0.9 mL of 0.1 M potassium phosphate (pH 7.0), 1 mM EDTA, and 100 $\mu$M NADPH containing a known amount of enzyme at 25 °C and following the decrease in absorbance at 340 nm. The enoyl reductase activity was measured similarly, except that 20 $\mu$L of 18.9 mM crotonyl-CoA, instead of acetoacetyl-CoA, was added to the assay mixture.

*Synthesis of Spin-Labeled $NADP^+$.* $NADP^+$ was covalently linked with the spin-label 2,2,5,5-tetramethyl-1-oxy-3-pyrroline-3-carboxylic acid by modification of the procedure of Guillory and Jeng (1977). Under an atmosphere of dry nitrogen, [$^1H_{13}$,$^{14}N$]- or [$^2H_{13}$,$^{15}N$]-2,2,5,5-tetramethyl-1-oxy-3-pyrroline-3-carboxylic acid (18.4 mg, 0.1 mmol) and 1,1′-carbonyldiimidazole (69.2 mg, 0.4 mmol) were mixed in dry form, dissolved in 0.5 mL of dry dimethylformamide, and stirred at room temperature for 60 min. After the initial reaction, $NADP^+$ (84.4 mg, 0.1 mmol) dissolved in 2.5 mL of water was added to the mixture, and the reaction was allowed to proceed for 48 h. The reaction mixture was dried under reduced pressure. Water then was added to a total volume of 20 mL, and the pH of the solution was adjusted to 7.0 with 1 M HCl. The product was purified in 4-mL aliquots by anion-exchange chromatography on DEAE-Sephadex A-25 (acetate form, 1.5 × 46 cm) with a linear gradient of 1 L each of water and 0.4 M ammonium acetate (pH 7.0). Further purification was achieved by reverse-phase high-performance liquid chromatography on an Alltex 10 × 250 mm $C_{18}$ column.

The products were identified with ultraviolet spectroscopy, thin-layer chromatography, EPR, and nuclear magnetic resonance and in one case by mass spectrometry. Thin-layer chromatography was carried out on silica gel plates with three solvent systems: I, 2-propanol/1% aqueous ammonia sulfate (2:1 v/v); II, isobutyric acid/1 N $NH_4OH/H_2O$ (66:1:33 v/v/v); and III, 1-butanol/water/acetic acid (5:3:2 v/v/v). Nuclear magnetic resonance measurements were carried out on a Bruker WM300 and Varian XL200. Samples were prepared by dissolving the products in 99.9% $D_2O$ after the products were dried in a rotary evaporator and lyophilized twice from 99.9% $D_2O$. The mass spectrum was obtained by fast ion bombardment, after the sample was dissolved in thioglycerol, in the Middle Atlantic Mass Spectrometry Laboratory (The Johns Hopkins University, National Science Foundation Regional Instrumentation Facility). We are indebted to Dr. Richard van Breemen for carrying out this analysis.

The concentration of spin-labeled $NADP^+$ was determined with an extinction coefficient of $2.20 \times 10^4$ $M^{-1}$ $cm^{-1}$ at 260 nm.

*Inhibition of Fatty Acid Synthase.* The competitive inhibition constant of the spin-labeled $NADP^+$ was determined by steady-state kinetic measurements. Enzyme activity was

[1] Abbreviations: EPR, electron paramagnetic resonance; SL, (2,2,5,5-tetramethyl-1-oxy-3-pyrrolin-3-yl)carbonyl; EDTA, ethylenediaminetetraacetic acid; Tris, tris(hydroxymethyl)aminomethane; NADPH, reduced nicotinamide adenine dinucleotide phosphate; $NADP^+$, nicotinamide adenine dinucleotide phosphate; CoA, coenzyme A.

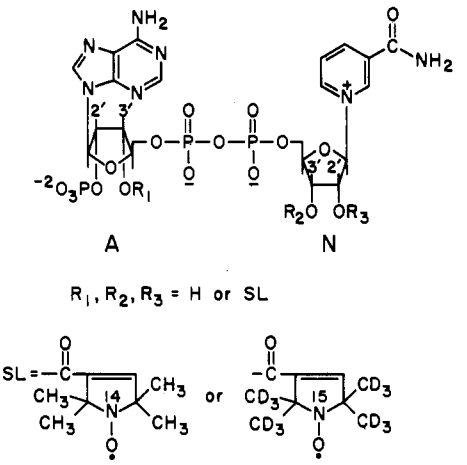


FIGURE 1: Structures of the spin-labeled NADP$^+$ reaction products.

measured spectrophotometrically with a Cary 2200 (Varian) spectrophotometer at 25 °C by monitoring the loss of NADPH at 340 nm. The assay mixture contained 100 mM potassium phosphate (pH 7.0), 1 mM EDTA, 100 $\mu$M malonyl-CoA, 50 $\mu$M acetyl-CoA, 2.2–11.1 $\mu$M NADPH, and 44.8–89.7 $\mu$M $N_{3'}$-O-SL-NADP$^+$. Before the start of the assay, the reaction mixture was incubated in the cuvette at 25 °C for 5 min.

*EPR Measurements.* EPR spectra were obtained with a Bruker ER-200D-SRC spectrometer at 9.6 or 9.4 GHz. Both microwave power and modulation amplitude were chosen to be below the onset of broadening. The scan speed and time constant were adjusted to avoid any artifact from scanning (Jost & Griffith, 1978). The microwave power was 6.3 or 10.1 mV, and the modulation frequency was 100 kHz with an amplitude of 0.1 or 0.8 G. For low-temperature studies, the sample was introduced into the $TM_{4103}$ cavity, and the temperature was maintained and measured with a Bruker ER 4111 variable temperature unit. All samples were in a capillary tube [(1.6–1.8) × 100 mm]. Time averaging was done with an IBM system 9000 microcomputer, which was employed to drive the spectrometer's magnetic field and to record signals digitally. Experimental data were replotted with a PDP 11/24 computer.

The rigid-limit EPR spectrum of enzyme-bound spin-labeled NADP$^+$ at −50 or −80 °C was obtained to determine all elements of the nitrogen hyperfine (**A**) and electron–Zeeman (**g**) tensors that are required as input for computing rotational correlation times. The amount of bound label was 0.7 or 1.9 mol/mol of enzyme at 25 °C. The spectral simulations for finding **A** and **g** tensors and for calculating rotational correlation times were carried out with the algorithm of Freed (1976).

## RESULTS

*Characterization of Reaction Products.* The reaction products of interest are shown in Figure 1. After reaction of NADP$^+$ with 2,2,5,5-tetramethyl-1-oxy-3-pyrroline-3-carboxylic acid, seven peaks were detected by anion-exchange chromatography on DEAE-Sephadex A-25 (Figure 2): two of starting material (peaks I and VII) and five of reaction products (peaks II–VI). Peaks I and VII were identified as the starting materials, spin-label, and NADP$^+$, respectively. The reaction products (peaks II–VI) gave an ultraviolet absorption spectrum with a maximum at 259 nm, indicating that no esterification had taken place at the 6-amino group of the adenine ring.

The major product peak (VI) eluted after 1236 mL of the water–ammonium acetate gradient and was lyophilized. This peak had an $R_f$ value of 0.32 (system I), 0.38 (system II), and

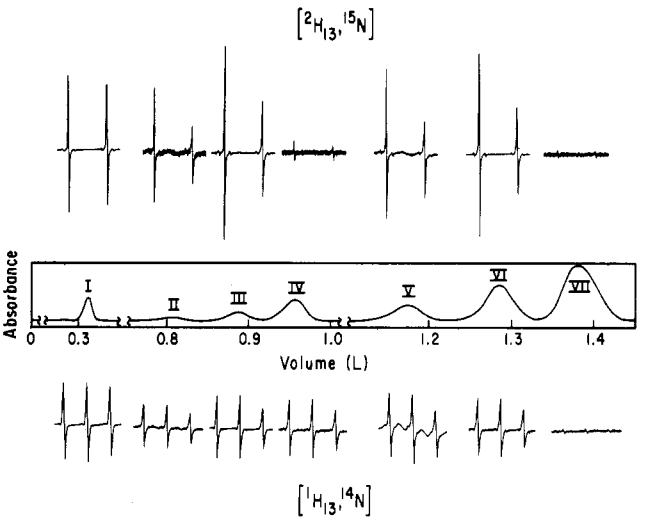


FIGURE 2: DEAE-Sephadex A-25 chromatography of the reaction products. The absorbance at 280 nm (full scale = 0.5 absorbance unit) vs. the elution volume (L) is shown. All separations were performed at 4 °C in a column (1.5 × 46 cm) equilibrated with 1 M ammonium acetate (pH 7.0). A linear gradient of 1 L each of water and 0.4 M ammonium acetate (pH 7.0) was used. EPR spectra of the reaction products (peaks I–VII) are also shown at the top and bottom of the chromatogram.

0.11 (system III) on silica gel plates. The ultraviolet spectrum showed maxima at 259 nm, due to the adenine ring, and at 210 nm, due to the $\alpha,\beta$-unsaturated carbonyl group. The EPR spectrum showed the expected triplet ($^{14}$N) or doublet ($^{15}$N) with a slightly broadened high-field line, typical of spin-labeled molecules of high molecular weight (Figure 2). Further purification of this material was achieved by reverse-phase high-performance liquid chromatography on an Alltex $C_{18}$ column with either a linear gradient of 10 mM ammonium acetate (pH 5.0)–methanol preceded by a 24-min equilibration with 98% ammonium acetate or a stepwise elution with 10 mM ammonium acetate (pH 5.0)–10% methanol (20 min), 15% methanol (32 min), and 40% methanol (8 min) at a flow rate of 2 mL/min. Three peaks were obtained. The first was unreacted NADP$^+$, which was identified by its rapid reduction to NADPH in the presence of 4.1 × 10$^{-5}$ M glucose 6-phosphate, 6.2 × 10$^{-5}$ M $MgCl_2$, and glucose-6-phosphate dehydrogenase and by its $R_f$ value on silica gel thin-layer chromatography. The two product species, present in a proportion of about 10% and 90%, had identical ultraviolet spectra, $R_f$ values on silica thin-layer plates, and EPR spectra. The more prevalent species probably is the $N_{3'}$ ester and the other the $N_{2'}$ ester (see Discussion; Profy & Usher, 1984; Guillory et al., 1980). After lyophilization, the $N_{3'}$ ester peak was further characterized with NMR and mass spectrometry. The NMR spectrum indicated the presence of the adenine and nicotinamide ring, but with broadened peaks due to the paramagnetic nitroxide. Mass spectrometry revealed two major species: a molecular ion, [MH]$^+$, with a mass to charge ratio of 910 and the corresponding positively charged molecular ion with a mass of charge ratio of 909. The thioglycerol adduct with a mass to charge ratio of 1017 confirmed the molecular weight of 909. A molecular weight of 909 corresponds to the calculated molecular weight of $N_{3'}$-O-[$^1H_{13}$,$^{14}$N]SL-NADP$^+$, $N_{2'}$-O-[$^1H_{13}$,$^{14}$N]SL-NADP$^+$, or $A_{3'}$-O-[$^1H_{13}$,$^{14}$N]SL-NADP$^+$. The first of these species is the actual product. The other two are minor products of the reaction mixture, the minor species in peaks VI and III, respectively.

Peak V, eluted after 1120 mL of the water–ammonium acetate gradient, was lyophilized. It has an $R_f$ value of 0.29

(system I), 0.43 (system II), and 0.19 (system III) on the silica gel plates. The ultraviolet spectrum showed maxima at 210 and 259 nm. The EPR spectrum has five lines for $^1H_{13},^{14}N$ spin-label, or three lines for $^2H_{13},^{15}N$ spin-label, that show the appearance of additional lines between the components of the typical triplet, or doublet, spectrum characteristic of the mononitroxyls (Figure 2). If the temperature is increased to 52 °C, the additional lines increase in amplitude due to the electron–electron exchange interaction of the dinitroxide spin-labeles (Calvin et al., 1969; Rozantsev, 1970). This species was further characterized after purification by high-performance liquid chromatography, as with peak VI. The NMR spectrum of the major species indicated the resolved protons of both the adenine and nicotinamide ring, with the spectrum broader than that of the $N_{3'}$ spin-label because of the dinitroxide. The distance between the nitroxide radicals was calculated from the EPR dipole–dipole splitting (85.5 G at −56 °C) and was about 8–9 Å {$r$ (Å) = [(5.56 × $10^4$)/maximum splitting (G)]$^{1/3}$; Jost & Griffith, 1978}. The crystal structure of the (+)-3-carboxy-2,2,5,5-tetramethyl-1-pyrrolidinyloxy (Lajzerowicz-Bonneteau, 1976) indicates that this product must be $N_{2'},N_{3'}$-O-bis-SL-NADP$^+$. The relative mole ratio of peak VI to peak V is about 2.

The remaining three peaks (II–IV) represent about 30% of the reaction products. The properties and structures of these peaks have not been determined in detail, but they can be assigned as $A_{3'},N_{2'}(N_{3'})$-O-bis-SL-NADP$^+$, $A_{3'}$-O-SL-NADP$^+$, and unknown products, respectively. Relative to the spectrum of peak V (Figure 2), the EPR spectrum of peak II shows two additional weaker lines for $^1H_{13},^{14}N$, or one for $^2H_{13},^{15}N$, spin-label. Thus, a weaker electron–electron interaction occurs than for the $N_{2'},N_{3'}$-O-bis-SL-NADP$^+$, indicating the distance between nitroxides is greater than 8–9 Å. The EPR spectrum of peak III shows a triplet and doublet for $^1H_{13},^{14}N$ and $^2H_{13},^{15}N$ spin-labels, respectively (Figure 2). This means that the species contains a single spin-label. The most likely binding site is the AMP portion of NADP$^+$. The relative mole ratio of peaks III and VI is 0.2. The relatively small amount of the $A_{3'}$ ester is due to restricted access to the reactive site caused by the 2′-phosphate of NADP$^+$. Peak IV represented about 20% of the total products and showed a very weak EPR signal (Figure 2).

The EPR spectrum of $N_{3'}$-O-[$^2H_{13},^{15}N$]SL-NADP$^+$ displayed about a 2.7-fold decrease in line width and a 5-fold increase in amplitude (low-field line) as compared to that of $N_{3'}$-O-[$^1H_{13},^{14}N$]SL-NADP$^+$ (Figure 3). The improvement in amplitude is due to both the reduction in the number of EPR lines from three (for $^{14}N$) to two (for $^{15}N$) and the decreased line width. This enhancement in amplitude is similar to that observed with $^{15}N$ perdeuterated spin-labeled NAD$^+$ (Philipp et al., 1984). The EPR spectra of $N_{2'},N_{3'}$-O-bis[$^2H_{13},^{15}N$]-SL-NADP$^+$ displayed about a 1.8-fold decrease in line width and a 1.6-fold increase in EPR signal amplitude (low-field line) as compared to the corresponding $^{14}N$ protonated analogue (data not shown).

*Inhibition of Fatty Acid Synthase by Spin-Labeled NADP$^+$.* Steady-state kinetic studies of fatty acid synthase show that $N_{3'}$-O-[$^1H_{13},^{14}N$]SL-NADP$^+$ is a competitive inhibitor of NADPH. Some typical results are shown in Figure 4. For competitive inhibition

$$v/[E_0] = (k_{cat}[NADPH]/K_N)/(1 + [NADPH]/K_N + [SL\text{-}NADP^+]/K_I) \quad (1)$$

where $v$ is the steady-state initial velocity, $k_{cat}$ is the apparent turnover number, $[E_0]$ is the total enzyme concentration, $K_N$ is the apparent Michaelis constant for NADPH, and $K_I$ is the inhibition constant for SL-NADP$^+$. The concentrations of acetyl-CoA and malonyl-CoA are constant. A least-squares analysis of the data gives $K_I$ = 133 ± 20 μM at 25 °C.

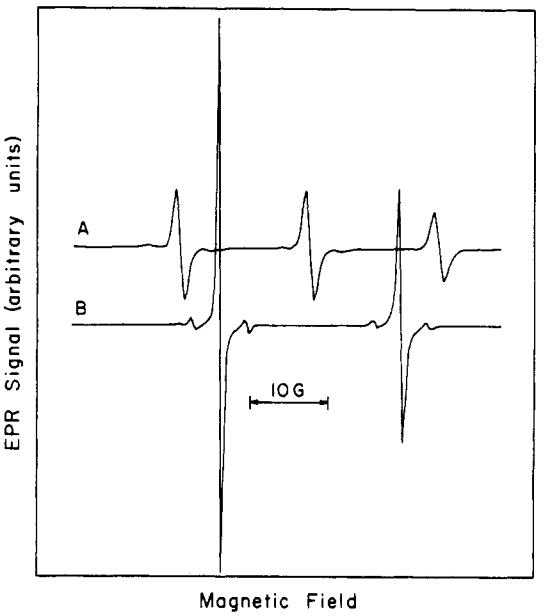


FIGURE 3: EPR spectra of $N_{3'}$-O-[$^1H_{13},^{14}N$]SL-NADP$^+$ (A) and $N_{3'}$-O-[$^2H_{13},^{15}N$]SL-NADP$^+$ (B). The spectra were obtained with 200 μM spin-label in 0.1 M potassium phosphate and 1 mM EDTA (pH 7.0) at 25 °C and were recorded at 10.1-mV microwave power with a modulation amplitude of 0.1 G. The two very small peaks on either side of each of the two main EPR lines of (B) are due to natural abundance $^{13}C$ adjacent to the N–O moiety.

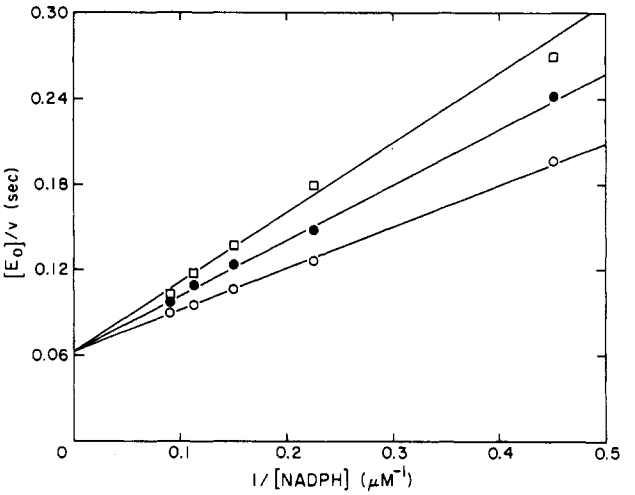


FIGURE 4: A plot of $[E_0]/v$ vs. $1/[NADPH]$ for fatty acid synthase, where $[E_0]$ is the total enzyme concentration and $v$ the steady-state initial velocity. The assay mixture contained 0.1 M potassium phosphate (pH 7.0), 1 mM EDTA, 100 μM malonyl-CoA, 50 μM acetyl-CoA, 2.2–11.1 μM NADPH, and 0.0 (○), 44.8 (●), or 89.7 (□) μM $N_{3'}$-O-[$^1H_{13},^{14}N$]SL-NADP$^+$ at 25 °C. The solid lines are the best fit of the data to eq 1 with $k_{cat}$ = 15.7 $s^{-1}$, $K_N$ = 8.0 μM, and $K_I$ = 133 μM.

*EPR Titration of Enzyme with Spin-Labeled NADP$^+$.* $N_{3'}$-O-[$^1H_{13},^{14}N$]SL-NADP$^+$ and $N_{3'}$-O-[$^2H_{13},^{15}N$]SL-NADP$^+$ have the typical three- and two-line EPR spectra expected for a paramagnetic nitroxide, respectively. In the presence of fatty acid synthase, a decrease in the intensity of the EPR signal occurred due to the binding of the spin-labeled NADP$^+$ to the enzyme. At a [spin-labeled NADP$^+$]/[fatty acid synthase] ratio of ≥1 per dimer and a low concentration of the fatty acid synthase, no significant changes in the line shape of the spectrum were observed because the spectrum

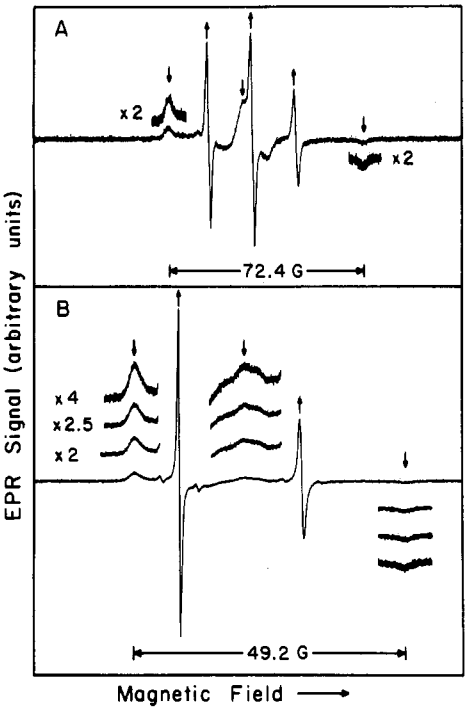


FIGURE 5: EPR spectra of $N_{3'}$-O-[$^1H_{13}$,$^{14}N$]SL-NADP$^+$ (A) and $N_{3'}$-O-[$^2H_{13}$,$^{15}N$]SL-NADP$^+$ (B). The EPR spectra were obtained with 307 $\mu$M spin-labeled NADP$^+$ and 287 $\mu$M fatty acid synthase (A) or with 254 $\mu$M spin-labeled NADP$^+$ and 293 $\mu$M fatty acid synthase (B) in 0.1 M potassium phosphate (pH 7.0) and 1 mM EDTA at 25 °C. The spectra show two types of EPR signals: the sharp lines are due to unbound spin-labeled NADP$^+$ (marked as ↑), and the broad lines are due to bound spin-labeled NADP$^+$ (marked as ↓). Approximately 1 mol of ligand is bound per mole of enzyme.

is dominated by the signal of the unbound spin-labeled NADP$^+$. However, at a [spin-labeled NADP$^+$]/[fatty acid synthase] ratio of about 1 per dimer and a high concentration of fatty acid synthase (about 300 $\mu$M), an altered shape was observed due to the immobilization of the spin-label accompanying binding of spin-labeled NADP$^+$ to the enzyme. Typical spectra are shown in Figure 5 for $N_{3'}$-O-[$^1H_{13}$,$^{14}N$]-SL-NADP$^+$ and $N_{3'}$-O-[$^2H_{13}$,$^{15}N$]SL-NADP$^+$. The sharp lines are due to the unbound ligand and the broad lines to the bound ligand. Since the concentration of nitroxide spin-label varies as the product of the line width and height of the first-derivative line (Jost & Griffith, 1978), the spectral amplitude of unbound spin-labeled NADP$^+$ is dominant. The separation of the low-field maximum and high-field minimum for the bound $N_{3'}$-O-[$^1H_{13}$,$^{14}N$]SL-NADP$^+$ is 72.4 G, which is typical for highly constrained nitroxide spin-labels. For $N_{3'}$-O-[$^2H_{13}$,$^{15}N$]SL-NADP$^+$, this difference is 49.2 G. The middle peak of the bound species does not overlap the spectrum of the unbound spin-labeled NADP$^+$ in this latter case. The spectra of the bound ligands were completely abolished when a high concentration of NADPH (~2 mM) was added, indicating the binding is specific for the catalytic sites.

The enzyme was titrated with $N_{3'}$-O-[$^1H_{13}$,$^{14}N$]SL-NADP$^+$, and the concentration of free ligand was determined from the amplitude of the line at highest magnetic field, with the assumption that the contribution of the bound ligand to the amplitude can be neglected. A plot of the signal amplitude vs. the concentration of the spin-labeled ligand (160–457 $\mu$M) is shown in Figure 6. A similar plot in the presence of 25 $\mu$M enzyme also is presented. The titrations were carried out in 0.1 M potassium phosphate and 1 mM EDTA (pH 7.0) at 25 °C. The concentrations of free ligand can be calculated directly from the amplitude of the spectral line, and the

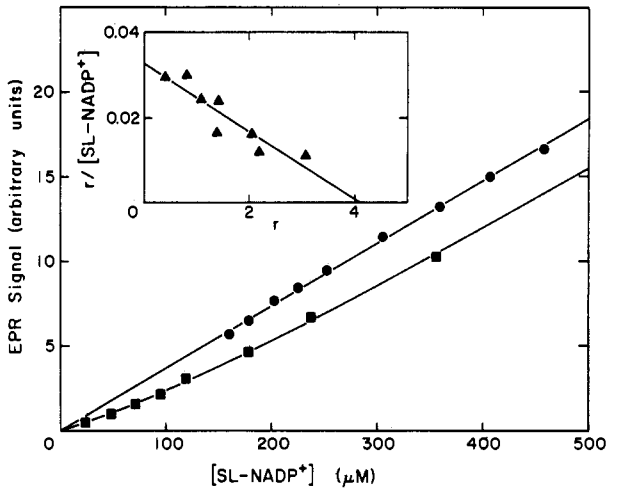


FIGURE 6: EPR titration of fatty acid synthase with $N_{3'}$-O-[$^1H_{13}$,$^{14}N$]SL-NADP$^+$ in 0.1 M potassium phosphate, pH 7.0, 1 mM EDTA, and 25.3 $\mu$M enzyme at 25 °C. A plot of the amplitude of the EPR peak at high field due to the unbound ligand in the absence (●) and presence (■) of 25.3 $\mu$M fatty acid synthase is shown. The inset is a plot of $r/[L]$ vs. $r$ obtained from the EPR data. Here, $r$ is the moles of ligand bound per mole of enzyme, and [L] is the concentration of unbound ligand. The solid line of the inset plot has been calculated with the best-fit parameters to eq 2: $K = 124 \pm 22$ $\mu$M and $n = 4.08 \pm 0.48$. The curve in the presence of enzyme has been calculated with these constants and the proportionality constant obtained from the data in the absence of enzyme.

concentration of bound ligand can be calculated from the known total concentration of ligand. These data were used to construct the Scatchard plot (Scatchard, 1949) in the inset of Figure 6, which was analyzed according to

$$r/[L] = n/K - r/K \quad (2)$$

Here, $r$ is the moles of ligand bound per mole of enzyme, [L] is the concentration of unbound ligand, $K$ is the dissociation constant, and $n$ is the number of binding sites per mole of enzyme. A linear least-squares analysis gives $K = 124 \pm 22$ $\mu$M and $n = 4.08 \pm 0.48$. The curve in Figure 6 has been calculated with these constants and the proportionality constant obtained from the data in the absence of enzyme.

Since fatty acid synthase has multiple binding sites, the possibility of electron–electron dipolar interactions between bound spin-labeled NADP$^+$ molecules exists. If such interactions are present, new spectral lines at high and low magnetic fields would be observed when all four binding sites per enzyme molecule are occupied. For the spectra in Figure 5, approximately 1 binding site per enzyme molecule is occupied. The spectra obtained when approximately four binding sites per enzyme molecule are occupied by the spin-label are shown in Figure 7. By necessity, the fraction of the ligand bound is less than in Figure 5. However, the spectra of the bound ligands are unchanged, and no evidence for dipolar interactions could be found. This indicates that the distance between bound nitroxides is greater than about 15 Å (Beth et al., 1984; Calvin et al., 1969) and that the environments of the four binding sites around the spin-label produce indistinguishable spectra.

Further investigation of the binding sites was carried out by modification of the enzyme with pyridoxal 5′-phosphate (Poulose & Kolattukudy, 1980; Cardon & Hammes, 1983). This blocks the binding of NADPH to the enoyl reductase sites and eliminates the enoyl reductase activity. The EPR spectrum of ~1.8 $N_{3'}$-O-[$^2H_{13}$,$^{15}N$]SL-NADP$^+$ bound per enzyme molecule was identical with that of the native enzyme, indicating no significant differences between the spin-label environments of the $\beta$-ketoacyl reductase and enoyl reductase

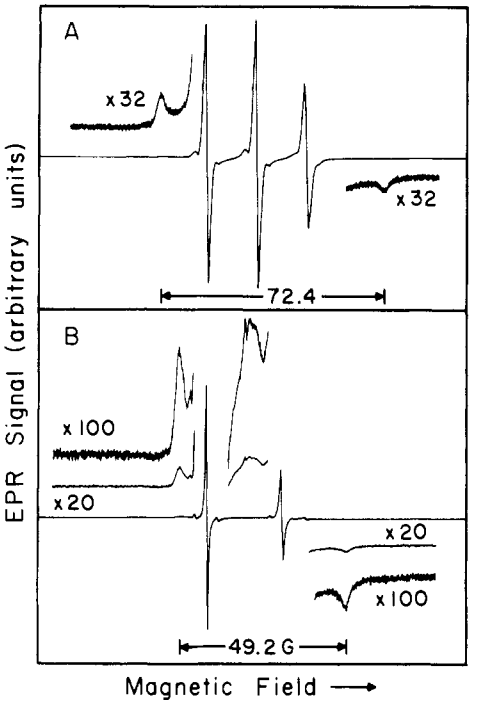


FIGURE 7: EPR spectra of $N_{3'}$-O-[$^1H_{13}$,$^{14}N$]SL-NADP$^+$ (A) and $N_{3'}$-O-[$^2H_{13}$,$^{15}N$]SL-NADP$^+$ (B). The EPR spectra were obtained with 2.50 mM spin-labeled NADP$^+$ and 239 $\mu$M enzyme (A) or with 2.53 mM spin-labeled NADP$^+$ and 272 $\mu$M enzyme (B) in 0.1 M potassium phosphate (pH 7.0) and 1 mM EDTA at 25 °C. Approximately four binding sites per enzyme molecule are occupied by the spin-labeled NADP$^+$.

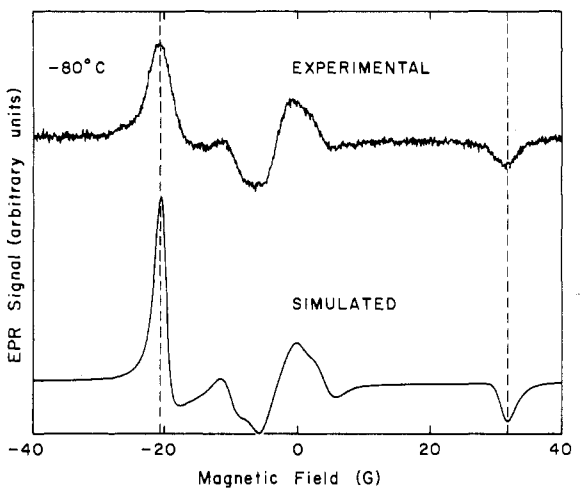


FIGURE 8: Experimental and simulated EPR spectra of 64 $\mu$M $N_{3'}$-O-[$^2H_{13}$,$^{15}N$]SL-NADP$^+$ with 141 $\mu$M fatty acid synthase in 0.1 M potassium phosphate (pH 7.0), 1 mM EDTA, and 50% glycerol (v/v) at −80 °C. The calculation of the simulated EPR spectrum is described in the text. The values of the electron–Zeeman (**g**) and nitrogen hyperfine (**A**) tensors in Table I were determined from the simulated spectrum.

binding sites. No evidence for dipolar interactions was found.

The fatty acid synthase also was dissociated into monomers at 4 °C. The overall fatty acid synthase activity was eliminated, but both the $\beta$-ketoacyl reductase and enoyl reductase were fully active. With ~1.8 $N_{3'}$-O-[$^2H_{13}$,$^{15}N$]SL-NADP$^+$ bound per enzyme molecule, the EPR spectrum of the bound ligand was not significantly altered relative to spectra obtained with the native enzyme. The outer hyperfine splitting was increased to 51.8 G because of the lower temperature; this indicates a slightly more restricted motion of the bound nitroxide.

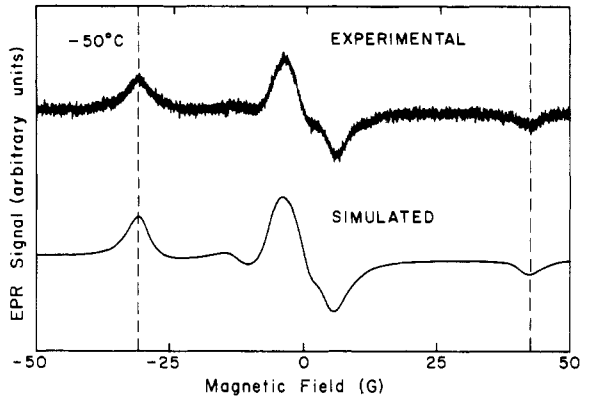


FIGURE 9: Experimental and simulated EPR spectra of 87 $\mu$M $N_{3'}$-O-[$^1H_{13}$,$^{14}N$]SL-NADP$^+$ with 95 $\mu$M fatty acid synthase in 0.1 M potassium phosphate (pH 7.0), 1 mM EDTA, and 50% glycerol (v/v) at −50 °C. The calculation of the simulated EPR spectrum is described in the text. The values of the electron–Zeeman (**g**) and nitrogen hyperfine (**A**) tensors in Table I were determined from the simulated spectrum.

Some preliminary experiments were also carried out with the doubly spin-labeled NADP$^+$, $N_{2'}$,$N_{3'}$-O-bis[$^2H_{13}$,$^{15}N$]SL-NADP$^+$. Although the spectrum of a double spin-label is more complex than that of a single spin-label, greater sensitivity to electron–electron interactions is possible (Morrisett, 1976). However, the EPR spectrum of the enzyme-bound doubly spin-labeled NADP$^+$ is essentially identical with that for one or four bound ligands per enzyme molecule.

*Rotational Correlation Times of Enzyme-Bound Spin-Labeled NADP$^+$.* The rotational correlation time for the enzyme-bound spin-label can be obtained by computer simulation of EPR line shapes (Freed, 1976). In order to do this, the electron–Zeeman (**g**) and nitrogen hyperfine (**A**) tensors must be obtained from the rigid-limit spectra. The rigid-limit spectra for enzyme-bound $N_{3'}$-O-[$^2H_{13}$,$^{15}N$]SL-NADP$^+$ and $N_{3'}$-O-[$^1H_{13}$,$^{14}N$]SL-NADP$^+$ are shown in Figures 8 and 9, respectively. The spectra were obtained in 50% glycerol (v/v), 0.1 M potassium phosphate, and 1 mM EDTA (pH 7.0) at −80 and −50 °C, respectively. The simulated spectra for a Brownian motion model of isotropic rotational diffusion (Freed, 1976) calculated with the parameters in Table I are included in Figures 8 and 9. For the $^2H_{13}$,$^{15}N$ spin-label an intrinsic Gaussian line broadening of 1.0 G was assumed, whereas for the $^1H_{13}$,$^{14}N$ spin-label a line broadening of 2.5 G was used. The rotational correlation times were $2.2 \times 10^{-7}$ and $1.2 \times 10^{-7}$ s, respectively. Spectra of enzyme-bound $N_{3'}$-O-[$^2H_{13}$,$^{15}N$]SL-NADP$^+$ were obtained over the temperature range −80 to 45 °C; they could be simulated with the parameters in Table I and the rotational correlation times in Table II. The correspondence between calculated and observed spectra is very good, similar to that found in Figure 8. Above 45 °C, the EPR spectrum deteriorated, probably due to denaturation of the enzyme. The rotational correlation times obtained are summarized in Table II. An activation energy of 2.3 kcal/mol can be calculated from these data.

To examine the effect of glycerol on the rotational correlation times, spectra of bound $N_{3'}$-O-[$^2H_{13}$,$^{15}N$]SL-NADP$^+$ were examined in 5 mM Tris, 35 mM glycine, and 1 mM EDTA (pH 8.3) over the temperature range −80 to 4 °C. Computer simulations were carried out as above. Although the solution went from solid to liquid, the rotational correlation times differ only slightly from those obtained in glycerol (Table II). An activation energy of 2.5 kcal/mol was calculated from these data. The rigid-limit **g** and **A** tensors are included in Table I.

Table I: Values of the Rigid-Limit Electron–Zeeman (g) and Nitrogen Hyperfine (A) Tensors

| compd | $g_{xx}$ | $g_{yy}$ | $g_{zz}$ | $A_{xx}$ (G) | $A_{yy}$ (G) | $A_{zz}$ (G) |
|---|---|---|---|---|---|---|
| [$^1H_{13}$,$^{14}N$]SL-NADP$^+$ ($N_{3'}$ ester) | 2.0091 | 2.0062 | 2.0023 | 6.4 | 6.4 | 37.0[a] |
| [$^2H_{13}$,$^{15}N$]SL-NADP$^+$ ($N_{3'}$ ester | 2.0091 2.0087 | 2.0062 2.0062 | 2.0023 2.0013 | 7.6 6.1 | 7.6 7.1 | 53.4[a] 55.4[b] |

[a] 0.1 M potassium phosphate, 1 mM EDTA (pH 7.0), and 50% glycerol (v/v). [b] 5 mM Tris, 35 mM glycine, and 1 mM EDTA (pH 8.3).

Table II: Rotational Correlation Times of Enzyme-Bound $^2H_{13}$,$^{15}N$ Spin-Labeled NADP$^+$

| conditions | temp (°C) | $\tau_R$ (s) |
|---|---|---|
| 0.1 M potassium phosphate, 1 mM EDTA (pH 7.0), and 50% glycerol (v/v) | −80 | $2.20 \times 10^{-7}$ |
| | −50 | $1.20 \times 10^{-7}$ |
| | −23 | $6.40 \times 10^{-8}$ |
| | 4 | $3.20 \times 10^{-8}$ |
| | 25 | $2.74 \times 10^{-8}$ |
| | 35 | $2.62 \times 10^{-8}$ |
| | 45 | $2.51 \times 10^{-8}$ |
| 5 mM Tris, 35 mM glycine, and 1 mM EDTA (pH 8.3) | −80 | $2.20 \times 10^{-7}$ |
| | −50 | $1.20 \times 10^{-7}$ |
| | −23 | $5.01 \times 10^{-7}$ |
| | −13 | $4.14 \times 10^{-7}$ |
| | 4 | $3.20 \times 10^{-8}$ |

## Discussion

Although the synthesis of spin-labeled NADP$^+$ by use of 1,1′-carbonyldiimidazole has been previously reported (Guillory & Jeng, 1977), the reaction products have not been characterized. In fact, a complex mixture of products is obtained, and the relative amount of each product depends on the time of reaction and the molar ratio of the starting materials, NADP$^+$ and the nitroxide spin-label. The conditions reported here optimize formation of NADP$^+$ modified with a single nitroxide. If the reaction time is shortened to 4–6 h, essentially no NADP$^+$ modified with two spin-labels is formed, but a considerable amount of unreacted starting material remains. If the molar ratio of 2,2,5,5-tetramethyl-1-oxy-3-pyrroline-3-carboxylic acid to NADP$^+$ is greater than 4, over 95% of the products were peaks II and V (NADP$^+$ with two spin-labels).

The dimethylformamide/water solvent prevents reaction with the 6-amino group of adenine (Gottikh et al., 1970). The identification of the various products is straightforward, except for the specification of which isomer is the $N_{2'}$ ester and which is the $N_{3'}$ ester. Thermodynamic arguments suggest the $N_{3'}$ ester is the more stable of the two (Guillory et al., 1980; Profy & Usher, 1984). For our purposes, the most important point is that a single isomer was used in studying interactions of the spin-labeled ligand with the enzyme. However, the purification procedures used permit isolation of all of the singly and doubly spin-labeled NADP$^+$ derivatives.

The EPR studies of the binding of the spin-labeled NADP$^+$ to fatty acid synthase indicate four binding sites, as expected (Cognet et al., 1983). The dissociation constants obtained from direct binding, 124 μM, and from steady-state inhibition, 133 μM, are in good agreement. However, the dissociation constant for NADP$^+$ binding to the enzyme is considerably less: values of 11 μM (Srinivansan & Kumar, 1976) and 6.5 μM (Katiyar et al., 1975) have been reported. The dissociation constant for NADPH binding is 6 μM (Cognet et al., 1983). Evidently the spin-label severely alters the fit of NADP$^+$ to the catalytic sites.

The EPR spectra of the bound spin-labels are typical for rotationally restricted molecules. The binding environments for the spin-label of the β-ketoacyl reductase and enoyl reductase sites are indistinguishable by their EPR spectra. Similarly, breakdown of the enzyme into monomers does not alter the EPR spectra of bound spin-labeled NADP$^+$. The structures of the binding sites apparently are quite independent of this major structural change of the enzyme. Electron–electron dipolar interactions could not be observed under any conditions: native enzyme, monomeric enzyme, or pyridoxal 5′-phosphate modified enzyme. Bound $N_{3'}$-O-[$^2N_{13}$,$^{15}N$]SL-NADP$^+$ gave a better resolved spectrum than bound $N_{3'}$-O-[$^1N_{13}$,$^{14}H$]SL-NADP$^+$; however, electron–electron dipolar interactions were not observed for either compound. The use of NADP$^+$ with two spin-labels potentially provides greater sensitivity than NADP$^+$ with a single spin-label, but again the electron–electron interactions were absent. This clearly indicates the four binding sites are at least ~15 Å apart.

The simulation of the EPR spectra of the bound spin-labeled NADPH with a stochastic model for isotropic rotational diffusion (Freed, 1976) reproduced the experimental spectra well. The values of the nitrogen hyperfine and electron–Zeeman tensors could be obtained from the spectra at low temperatures and were quite similar for $N_{3'}$-O-[$^2H_{13}$,$^{15}N$]-SL-NADP$^+$ in the presence and absence of glycerol. The only significant difference between the simulated and experimental spectra was in the width of the peaks at −20 G for $N_{3'}$-O-[$^2H_{13}$,$^{15}N$]SL-NADP$^+$ and −30 G for $N_{3'}$-O-[$^1H_{13}$,$^{14}N$]SL-NADP$^+$: the experimental peak is consistently broader. This phenomenon has been observed before for spin-labeled NAD$^+$ (Phillip et al., 1984). The broadening cannot be attributed to electron–electron interactions between bound spin-labels since it is observed with only one spin-labeled NADP$^+$ bound per molecule, with the monomeric enzyme, and with the enoyl reductase binding sites blocked by pyridoxamine phosphate. The mechanism for this slight broadening remains to be elucidated.

The temperature dependence of the correlation times was determined for the enzyme-bound $N_{3'}$-O-[$^2H_{13}$,$^{15}N$]SL-NADP$^+$ in the presence and absence of glycerol. This particular combination of isotopes provides increased sensitivity, and the computer simulation time is less than with the $^1H_{13}$,$^{14}N$-labeled derivative. Since the rotational correlation times and activation energies do not differ significantly in the presence and absence of glycerol, the rotation must be localized on the enzyme surface. The rotational correlation time of the enzyme itself is about 600 ns at room temperature (Anderson & Hammes, 1983), which can be compared with an EPR rotational correlation time of 27 ns under comparable conditions.

In summary, a variety of spin-labeled NADP$^+$ derivatives have been prepared and characterized. $N_{3'}$-O-SL-NADP$^+$ binds specifically to four catalytic sites on fatty acid synthase. The bound spin-label undergoes restricted rotation on the surface of the enzyme, and the spin-label environment of all four sites is similar. No alterations in the environment of the spin-label are caused by interactions between the binding sites, which must be at least ~15 Å apart.

**Registry No.** NADPH, 53-57-6; NADP$^+$, 53-59-8; $N_{3'}$-O-[$^1H_{13}$,$^{14}N$]SL-NADP$^+$, 103303-89-5; $N_{3'}$-O-[$^2H_{13}$,N]SL-NADP$^+$, 103258-50-0; fatty acid synthase, 9045-77-6; [$^1H_{13}$,$^{14}N$]-2,2,5,5-tetramethyl-1-oxy-3-pyrroline-3-carboxylic acid, 2154-67-8; [$^2H_{13}$,$^{14}N$]-2,2,5,5-tetramethyl-1-oxy-3-pyrroline-3-carboxylic acid, 88168-79-0.

REFERENCES


Anderson, V., & Hammes, G. G. (1983) *Biochemistry 22*, 2995–3001.

Anderson, V., & Hammes, G. G. (1984) *Biochemistry 23*, 2088–2094.

Anderson, V., & Hammes, G. G. (1985) *Biochemistry 24*, 2147–2154.

Beth, A. H., Robinson, B. H., Cobb, C. E., Dalton, L. R., Trommer, W. E., Birktoft, J. J., & Park, J. H. (1984) *J. Biol. Chem. 259*, 9717–9728.

Calvin, M., Wang, H. H., Entine, G., Gill, D., Ferruti, P., Harpold, M. A., & Klein, M. P. (1969) *Proc. Natl. Acad. Sci. U.S.A. 63*, 1–8.

Cardon, J. W., & Hammes, G. G. (1983) *J. Biol. Chem. 258*, 4802–4807.

Cognet, J. A. H., & Hammes, G. G. (1985) *Biochemistry 24*, 290–297.

Cognet, J. A. H., Cox, B. G., & Hammes, G. G. (1983) *Biochemistry 22*, 6281–6287.

Cox, B. G., & Hammes, G. G. (1983) *Proc. Natl. Acad. Sci. U.S.A. 80*, 4233–4237.

Freed, J. H. (1976) *Spin Labeling: Theory and Applications* (Berliner, L. J., Ed.) Vol. I, pp 53–132, Academic Press, New York.

Gottikh, B. P., Krayevky, A. A., Tarussova, N. B., Purygin, P. P., & Tsilevich, T. L. (1970) *Tetrahedron 26*, 4419–4433.

Guillory, R. J., & Jeng, S. J. (1977) *Methods Enzymol. 46*, 259–288.

Guillory, R. J., Jeng, S. J., & Chen, S. (1980) *Ann. N.Y. Acad. Sci. 346*, 244–279.

Hammes, G. G. (1985) *Curr. Top. Cell. Regul. 26*, 311–324.

Hsu, R. Y., & Yun, S.-L. (1970) *Biochemistry 9*, 239–245.

Jost, P., & Griffith, O. H. (1978) *Methods Enzymol. 49*, 369–418.

Katiyar, S. S., Cleland, W. W., & Porter, J. W. (1975) *J. Biol. Chem. 250*, 2709–2717.

Kumar, S., & Porter, J. W. (1971) *J. Biol. Chem. 246*, 7780–7789.

Lajzerowicz-Bonneteau, J. (1976) *Spin Labeling: Theory and Applications* (Berliner, L. J., Ed.) Vol. I, pp 239–249, Academic Press, New York.

Morrisett, J. D. (1976) *Spin Labeling: Theory and Applications* (Berliner, L. J., Ed.) Vol. I, pp 273–338, Academic Press, New York.

Penefsky, H. S. (1977) *J. Biol. Chem. 252*, 2891–2899.

Philipp, R., McIntyre, J. O., Robinson, B. H., Huth, H., Trommer, W., & Fleischer, S. (1984) *Biochim. Biophys. Acta 790*, 251–258.

Poulose, A. J., & Kolattukudy, P. E. (1980) *Arch. Biochem. Biophys. 201*, 313–321.

Profy, A. T., & Usher, D. A. (1984) *J. Mol. Evol. 20*, 147–156.

Rozantsev, E. G. (1970) *Free Nitroxyl Radicals*, Plenum Press, New York.

Scatchard, G. (1949) *Ann. N.Y. Acad. Sci. 51*, 660–672.

Srinivansan, K. R., & Kumar, S. (1976) *J. Biol. Chem. 251*, 5352–5360.

Tsukamoto, Y., Wong, H., Mattick, J. S., & Wakil, S. J. (1983) *J. Biol. Chem. 258*, 15312–15322.

Vernon, C. N., & Hsu, R. Y. (1984) *Biochim. Biophys. Acta 788*, 124–131.

Wakil, S. J., Stoops, J. K., & Joshi, V. C. (1983) *Annu. Rev. Biochem. 52*, 537–579.

Yuan, Z., & Hammes, G. G. (1985) *J. Biol. Chem. 260*, 13532–13538.

Yun, S., & Hsu, R. Y. (1972) *J. Biol. Chem. 247*, 2689–2698.